

SVPWM based DTC of Three Level Voltage fed Open End Winding Induction Motor

G.Satheesh, T. Bramhananda Reddy, Ch. Sai Babu

Abstract: A Space Vector Pulse Width Modulation (SVPWM) based Direct Torque Control (DTC) of Dual Inverter Fed Open End Winding Induction Motor is analyzed in this paper. A SVPWM based, 3 level phase voltages are generated with two individual two level inverters. In this method, first inverter pulses are generated normally and second inverter pulses are generated with 180 degrees phase shift. But at a particular state of switching first inverter is switched in all states and second inverter is clamped to that active state. In the next state of switching the second inverter is switched in all states and first inverter is clamped to corresponding active state. One inverter output is superimposed on the other inverter, resulting a 3-level line voltage waveform for the induction motor. The imaginary switching time concept is used in the proposed method. It does not require any procedures for calculation of regions in space voltage vector and angle calculations sector identification. The imaginary switching time greatly reduces the complexity of the algorithm. Simulation studies have been carried out for the proposed scheme and results are presented.

Keywords— DTC, Dual Inverter, NSHC Algorithm, OEWIM, SVPWM.

I. INTRODUCTION

The multi level inverters produce a high voltage output using the devices with standard voltages. One such a technique is cascading of two 2-level inverters. With this concept the same maximal 3 level voltage output can be achieved [1] as in the conventional 3-level inverter. The induction motors which are using the low and medium power level applications are later changed to high power level applications by feeding the 3 phase stator winding with two separate 2-level inverters. The DTC for the high power induction motors was proposed [2] two decades back. Numerous researches have been carried out on the DTC of the induction motor in the past years, and proposed number of control techniques for the Open End Winding Induction Motor drive. The work presented in [3] results in Torque and speed fluctuations with higher ripple in the stator current. Direct Self Control technique has been proposed for machine with open-end winding configuration [4]. But with the three level inverters on both ends leads to increment in cost and complexity. The open-end winding configuration has been proposed for high power electric vehicle/ hybrid electric vehicle (EV/HEV) propulsions systems. In [1] SVPWM

technique is used to control the output voltage of 2 inverters connected at both ends of the motor winding. It should be noted that the switching frequency capacity of both the inverters are same. In [6] and [7], the schemes proposed are complex due to identification of the region since the entire region is divided in 24 small regions or in to 7 small regions. In order to reduce the complexity of the sector/region identification, a method for open-end winding configuration is proposed with SVPWM using the concept of imaginary switching times [8-9]. It does not require any sector or sub-sector identification. It greatly simplifies the control strategy. Also, the switching frequency of both the inverters are same.

In this paper a scheme is proposed to produce a 3 level output voltage from 2 two level inverters connected in series for the DTC of the Induction motor drive.

II. OPEN-END WINDING INDUCTION MOTOR

A schematic of the open-end winding induction motor drive is shown in Fig.1. Two 2-level inverters, INV-I, feeds the three ends of the stator winding R Y B, and the INV-2 feeds the three ends R' Y' and B'. INV-1and INV-2 are connected to two separate dc sources with magnitude of $V_{dc}/2$ to avoid the zero sequence currents.

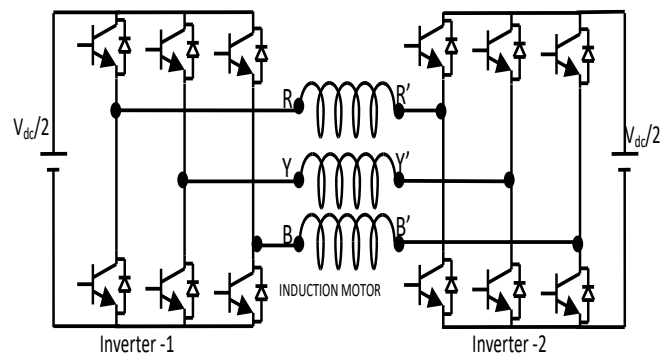


Fig 1: Open-end winding configuration of the Induction motor Drive

Fig. 2 represents the switching state vectors of two individual inverters and 3 level space vector combination. The conventional definition for the switching state sequences of the switches of phases of *ABC* of each individual inverter used here. In particular, for INV-1: **1 – 100; 2 – 110; 3 – 010; 4 – 011; 5 – 001; 6 – 101** (1 - switch-on state, 0 – switch-off state); and the same definition used for INV-2: **1' – 1'0'0'; 2' – 1'1'0'; 3' – 0'1'0'; 4' – 0'1'1'; 5' – 0'0'1'; 6' – 1'0'1'**, where 1' - switch-on state of switches of INV2, and 0' – switch-off state in INV-2. The pole voltages of INV-1 are V_{a0} , V_{b0} , V_{c0} and, the pole voltages of INV-2 are $V_{a'0}$, $V_{b'0}$, $V_{c'0}$. Any leg of the two inverters can independently attain levels 0 or $V_{dc}/2$.

Revised Manuscript Received on 30 November 2012.

* Correspondence Author

G. Satheesh is with the Department of EEE, G.P.R.E.C., Kurnool, Andhra Pradesh., India.

Dr. T. Bramhananda Reddy. is with the Department of EEE, G.P.R.E.C., Kurnool, Andhra Pradesh., India.

Dr. CH. Sai Babu is with the Electrical Engineering Department, J. N. T. U., Kakinada, Andhra Pradesh., India.

© The Authors. Published by Blue Eyes Intelligence Engineering and Sciences Publication (BEIESP). This is an open access article under the CC-BY-NC-ND license <http://creativecommons.org/licenses/by-nc-nd/4.0/>.

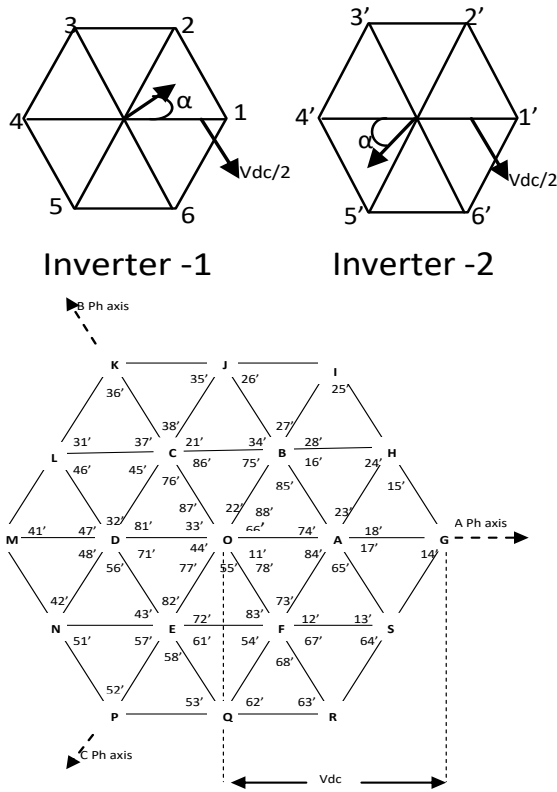


Fig 2: switching state vectors of two individual inverters and 3 level Generated Voltage Vectors

The voltage across a particular phase winding can be obtained by

$$V_{aa'} = V_{a0} - V_{a'0} \tag{1}$$

$$V_{bb'} = V_{b0} - V_{b'0} \tag{2}$$

$$V_{cc'} = V_{c0} - V_{c'0} \tag{3}$$

The effective phase voltages in the three windings can be represented by a voltage space vector as defined by

$$V_{ref} = V_{aa'} + V_{bb'}e^{j2\pi/3} + V_{cc'}e^{j4\pi/3} \tag{4}$$

This voltage space vector can be equivalently represented as the sum of the voltage space vectors generated by the two 2-level inverters and the 3 level output of the effective space phasor voltage that is represented in the figure 2 containing 64 vector locations with 24 sectors. Six adjacent sectors together form a hexagon. Six such hexagons can be identified with their centers located at A, B, C, D, E, and F respectively. In addition there is one inner hexagon with its center at O. Based on these sub-hexagons, a space phasor based PWM scheme is proposed in the same way as in the case of the conventional three phase inverter [10].

The switching algorithm described in reference [8] for a 2-level inverter feeding a conventional induction motor is extended for the dual-inverter system to compute the switching timings for individual inverters.

III. PROPOSED PWM STRATEGY

The algorithm specified in [8] uses only the instantaneous reference voltages and is based on the concept of ‘effective time’. The effective time is defined as the time “when the inverter supplies power to the motor in a given sampling time period and is denoted as T_{eff} . The sampling time period is denoted as T_s .

The instantaneous phase reference voltages are obtained by projecting the tip of the reference vector V_{sr} on to the respective phase axes and multiplying the values of these projections with a factor of (2/3). The factor (2/3) arises because of the classical ‘2 to 3 phase’ transformation. These instantaneous phase reference voltages are denoted as V_a^* , V_b^* and V_c^* . The symbols T_{ga} , T_{gb} and T_{gc} respectively denotes the time duration for which given motor phase is connected to the positive rail of the input DC power supply of the inverter in the given sampling time period T_s . The timings T_{ga} , T_{gb} and T_{gc} are termed as the phase switching times. The procedure to generate the gating pulses for the individual devices using this algorithm is elaborately explained in [11]. For a dual inverter system, there would be two sets of phase switching times, one for each inverter. The phase switching timings of inverter-1 are denoted by the symbols T_{ga} , T_{gb} and T_{gc} , while the symbols T'_{ga} , T'_{gb} and T'_{gc} denotes the same for inverter-2.

Few observations are made for the above strategies they are

1. To obtain the 3 level output first inverter output is superposed on the second inverter output at each vector location.
2. Hexagon ABCDEF with center O is named as core hexagon, there exist six outer hexagons namely OBHGSF, OCJIHA, ODLKJB, OENMLC, OFQPND and OASRQE centered around the points A, B, C, D, E and F respectively these are referred to as sub-hexagonal centers.
3. The space vector combinations at the vertices and at the center of a given sub- hexagon are obtained by clamping one inverter to a given state while the other inverter switches in all the eight states.

Alternate Inverter Switching Strategy

In this strategy we need to identify the nearest sub hexagonal centers and the corresponding center thereafter one inverter is switched and other inverter is clamped. In figure 3, to realize the 3 level reference voltage space vector OT, the OT vector is resolved into two switching vectors as OA and AT. Now, switch one inverter to generate the pulses to realize AT vector and the other inverter is clamped to OA vector. The net voltage impressed across the motor will be the vector sum of the two inverter voltage vectors. Table 1 summarizes the switching and clamping of inverters at different sub hexagonal centers.

Identification of nearest sub-hexagon centers:

If the tip of the reference vector lies inside the inner sub hexagon then center is chosen as O. If the tip of the reference vector lies outside of the inner sub hexagon then fig 4 illustrate the scheme for finding the sub hexagon center from the 3 phase reference sinusoid.

Table1: Clamping and switching of the inverters with respect to centers

Center	A	B	C	D	E	F
Inverter -I	Switching	Clamped to B	Switching	Clamped to D	Switching	Clamped to F
Inverter -II	Clamped to A	Switching	Clamped to C	Switching	Clamped to E	Switching

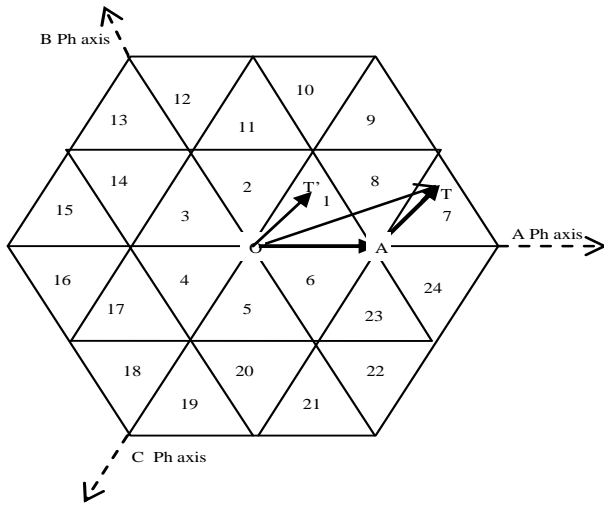


Fig 3: Reference space vector.

Let V_a , V_b and V_c represents the instantaneous magnitude of the 3 phase reference sinusoid. The sub hexagon centers of the outer sub hexagons are determined from the instantaneous magnitudes of V_a , V_b and V_c . For easy identification of the sub hexagon centers O is assigned with (000), A is assigned with (100), B is assigned with (110), C is assigned with (010), D is assigned with (011), E is assigned with (001), and F is assigned with (101) markings. If the magnitude of the sine wave is positive, it is represented as "1" and if the magnitude is negative, it is represented as "0". From figure 4(b), during the interval $\omega t=0$ to $\omega t=60$, V_a is positive, V_b is negative and V_c is positive, a sub hexagon center of F is marked. Similarly during the period of $\omega t=60$ to $\omega t=120$ V_a is positive. Therefore, the marking is obtained as (101) this corresponds to a sub hexagon center of F. Similarly during the period of $\omega t=60$ to $\omega t=120$ V_a is positive, V_b and V_c are negative which gives the marking as (100) this corresponds to a sub hexagon center of A. The above procedure is repeated to find the remaining sub hexagon centers. Therefore with the above specified procedure, no sector identification method is required to find the sector which contains the tip of the reference vector. As given is the Table 1 the identified sub hexagon center is used to drive the selected inverter.

Once the sub hexagon center is identified the co-ordinates of the corresponding center ($V_{\alpha nshc}$, $V_{\beta nshc}$) can be calculated [12]. The duration of the switching vectors is determined by shifting the outer sub hexagon to inner sub hexagon center A to coincide with the center of the inner sub hexagon center O [13]. Now the duration of the switching vectors can be determined by using the conventional equations for 2 level inverter [14]. If (V_α , V_β) are the co-ordinates of the instantaneous reference space vector OT, The new values of the co-ordinates of the switching inverters mapped to the OT' vector (Fig 4) are given by

$$\begin{aligned} V_{\alpha sw} &= V_\alpha - V_{\alpha nshc} \\ V_{\beta sw} &= V_\beta - V_{\beta nshc} \end{aligned} \quad (5)$$

The new phase values of mapped reference vector V_{as} , V_{bs} , V_{cs} are then calculated [14]. The switching timings T_{ga} , T_{gb} , and T_{gc} corresponding to the three phases are also computed as in [14].

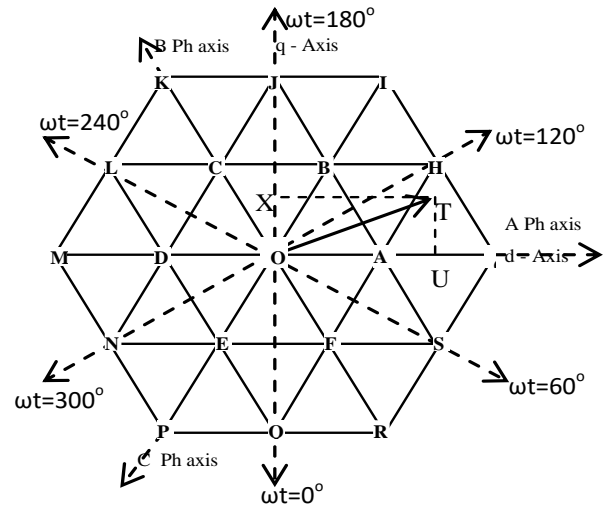


Fig 4(a): identification of sub hexagon centers

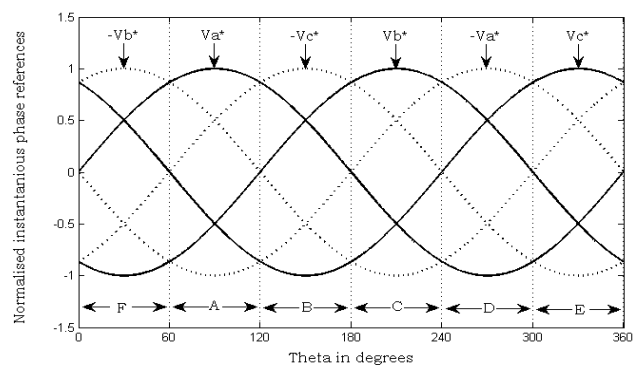


Fig 4(b): 3-phase reference signals and sub hexagon centers

IV. PROPOSED DTC OF OPEN END WINDING INDUCTION MOTOR DRIVE

From the basic principle, the DTC method selects one of the inverter's six voltage vectors and two zero vectors in order to keep the stator flux and torque within a hysteresis band around the demand flux and torque magnitudes. The torque produced by the induction motor can be expressed as,

$$T_e = \frac{3}{2} \frac{P}{L_s} \frac{L_m}{L_r} |\psi_s| |\psi_r| \sin \delta \quad (6)$$

This shows the torque produced is dependent on the stator flux magnitude, rotor flux magnitude, and the phase angle between the stator and rotor flux vectors. The induction motor stator equation,

$$\overline{V}_s = \frac{d\overline{\psi}_s}{dt} - \overline{I}_s R_s \quad (7)$$

can be approximated as

$$\Delta \overline{\psi}_s = \overline{V}_s \cdot \Delta t \quad (8)$$

Over a short time period if the stator resistance is ignored. From the above equations if a

voltage vector is applied that changes the stator flux to increase the phase angle between the stator flux and rotor flux vectors, then the torque produced will increase. The schematic of the proposed method is as shown in figure 5. In this method, speed of the reference stator flux vector $|\psi_s^*|$ is derived by the addition of slip speed and actual rotor speed. The actual synchronous speed of the stator flux vector $|\psi_s|$ is calculated from the adaptive motor model. After each sampling interval, actual stator flux vector $|\psi_s|$ is corrected by the error and it tries to attain the reference flux space vector $|\psi_s^*|$.

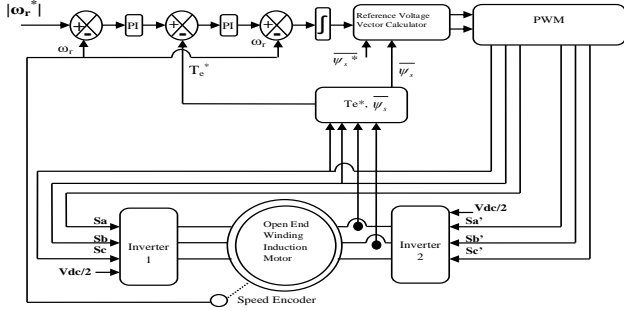


Fig 5: Block Diagram of the proposed method.

Thus the flux error is minimized in each sampling interval. In this paper, the direct axis and quadrature axis components of the reference voltage vector are created by corresponding direct axis and quadrature axes stator flux error components respectively. These are derived as follows: Reference value of the direct axis and quadrature axis stator fluxes and actual value of the direct axis and quadrature axis stator fluxes and are compared in the reference voltage vector calculator block and hence the error in the direct and quadrature axes stator flux vectors is obtained as

$$\Delta \psi_{ds} = \psi_{ds}^* - \psi_{ds} \quad (9)$$

$$\Delta \psi_{qs} = \psi_{qs}^* - \psi_{qs} \quad (10)$$

The knowledge of flux error and stator resistive drop allows the determination of appropriate reference voltage space vectors along direct axis and quadrature axis, which is given as

$$V_{ds}^* = R_s I_{ds} + \frac{\Delta \psi_{ds}}{T_s} \quad (11)$$

$$V_{qs}^* = R_s I_{qs} + \frac{\Delta \psi_{qs}}{T_s} \quad (12)$$

The above derived direct & quadrature components of the reference voltage vector are then fed to the SVPWM block, from where the gating pulses for two inverters are generated.

V. SIMULATION RESULTS

To validate the proposed method, simulation studies have been carried out by using MATLAB /SIMULINK. The motor parameters are as follows 4 KW, 400V, 30 N-m, 1470 rpm, 4-pole, 50 Hz, 3-phase, stator resistance $R_s = 1.57\Omega$, rotor resistance $R_r = 1.21\Omega$, stator inductance $L_s = 0.17H$, rotor inductance $L_r = 0.17H$, mutual inductance $L_m = 0.165H$,

moment of inertia $J = 0.089 \text{ Kg-m}^2$. It shows that three-level voltages are generated by two two-level inverters. Various conditions such as starting, steady state, step change in load and speed reversal are simulated. The reference flux is taken as 1 wb and starting torque is limited to 40 N-m . The simulation results for dual inverter fed DTC-IM drive are shown in from Fig 6 to Fig 16.

Fig 6 and Fig 7 show the no-load starting transients of speed, currents, torque, flux and phase and line voltages for AIS SVPWM algorithm based DTC-IM drive. The no-load steady state plots of speed, torque, stator currents, flux, phase and line voltages at 1200 rpm are given in Fig 8 –Fig 9.

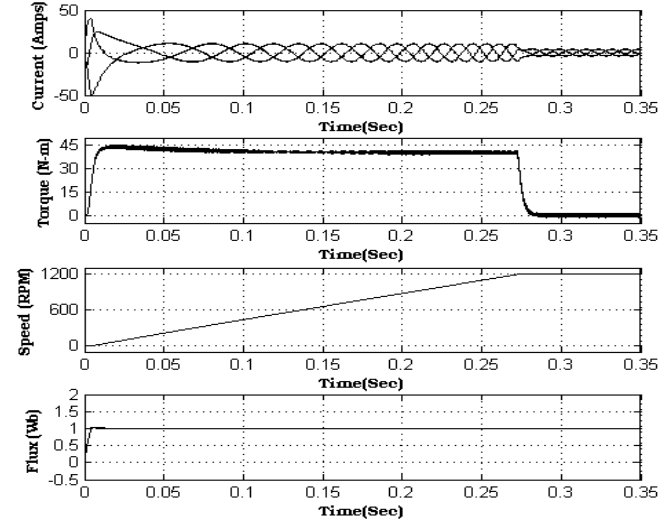


Fig 6: Starting transients of stator currents, torque, speed and stator flux for AIS-SVPWM-OEWIM drive

The harmonic distortion in the steady state stator current along with THD value is shown in Fig 14. From Fig 8 to Fig 9, it can be observed that the steady state ripple in torque, flux and current is very less compared to conventional DTC shown in Fig 17 and Fig 18.

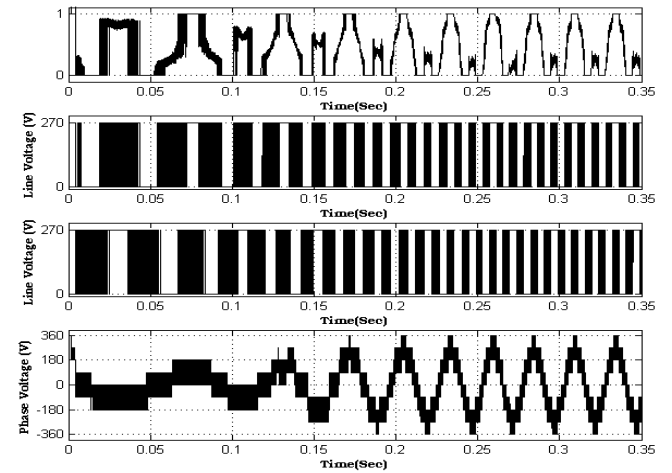


Fig 7: Starting transients in phase and line voltages of AIS-SVPWM-OEWIM drive

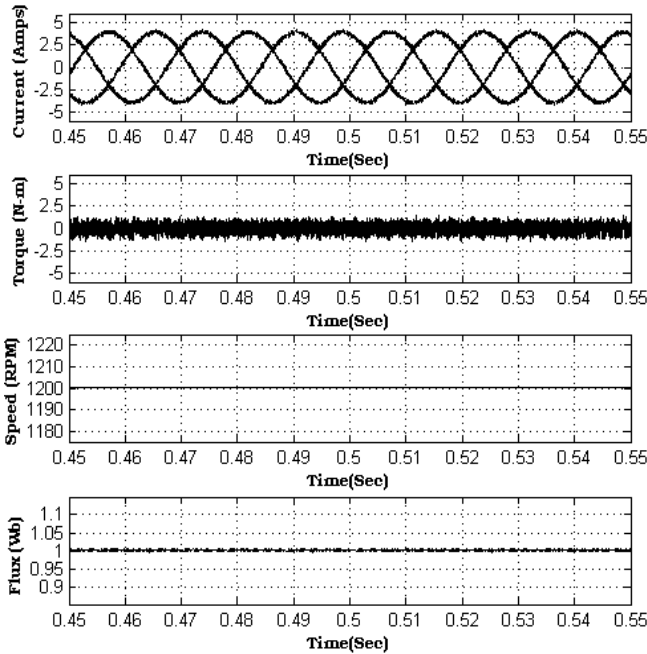


Fig 8: Steady state plots of stator currents, torque, speed and stator flux for AIS-SVPWM-IM drive at 1200 rpm

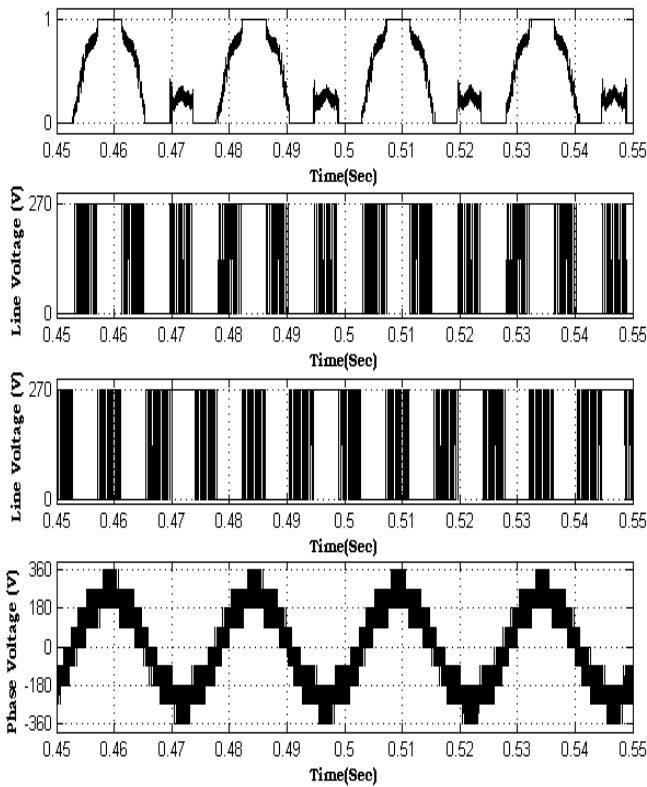


Fig 9: The phase and line voltages for AIS-SVPWM-OEWIM drive during the steady state

The proposed algorithm gives reduced THD in line current and voltages when compared with the decoupled PWM algorithm. Also, the proposed AIS SVPWM algorithm based DTC provides constant switching frequency of the inverter. Moreover, compared with the conventional DTC, the speed fluctuations can also be reduced. The locus of the stator flux is given in Fig 16. From which it can be observed that the locus is almost is a circle of constant radius.

The transients in speed, torque, currents and flux during the

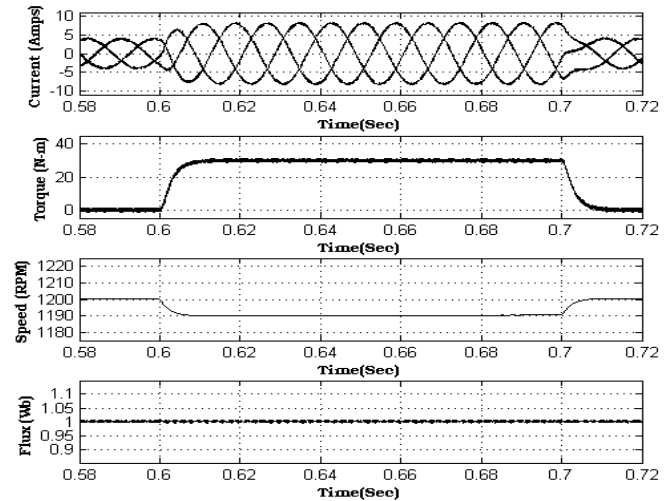


Fig 10: Transients in stator currents, torque, speed and stator flux during step change in load: a 30 N-m load is applied at 0.6 sec and removed at 0.7 sec

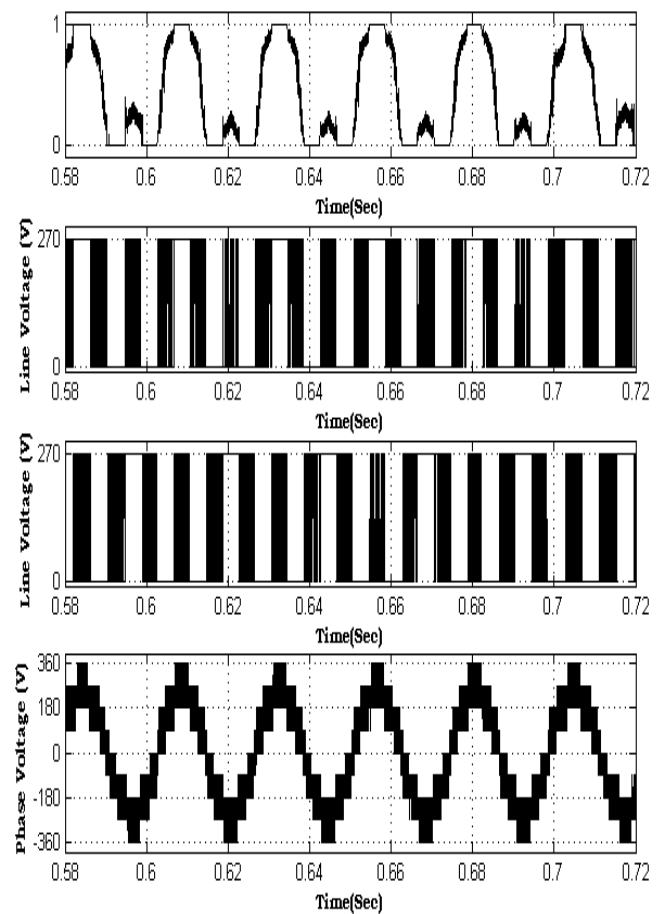


Fig 11: the phase and line voltages during a step change in load torque: a 30 N-m load torque is applied at 0.6 sec and removed at 0.7 sec

step change in load torque and corresponding phase and line voltages are shown in Fig 11. Also, the transients in speed, torque, currents, flux, and voltages during the speed reversals (from +1200 rpm to -1200 rpm) are shown from Fig 12.

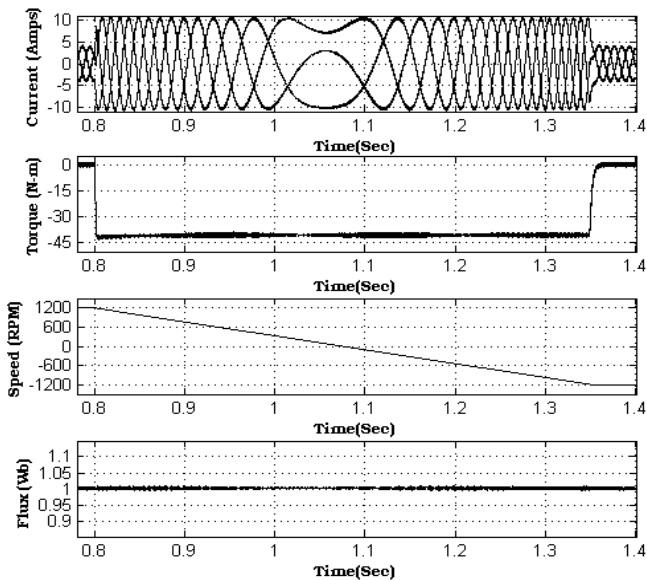


Fig 12: Transients in stator currents, torque, speed and stator flux during speed reversal: speed is changed from +1200 rpm to -1200 rpm at 0.8 s

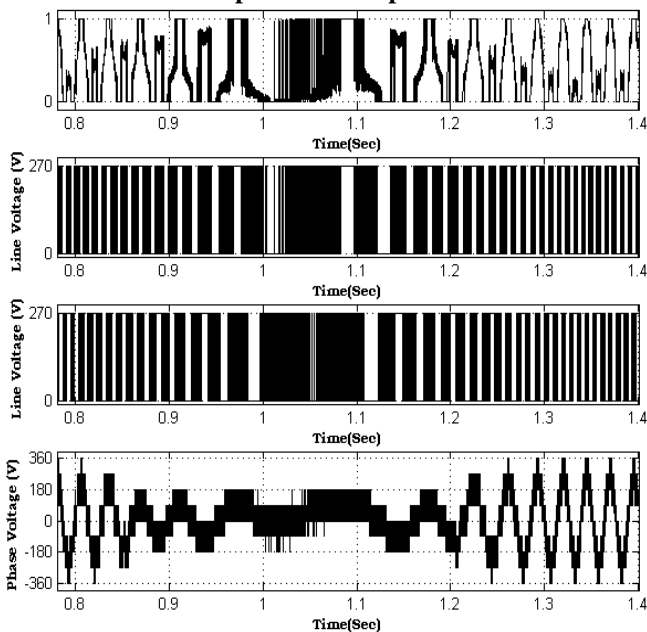


Fig 13: The phase and line voltage variations during the speed reversal (speed is changed from +1200 rpm to -1200 rpm at 0.8s)

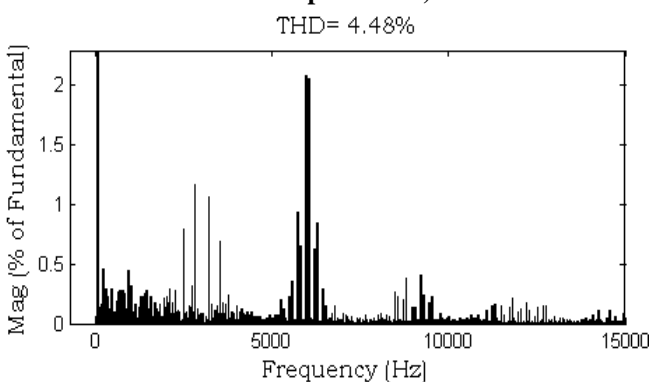


Fig 14: Harmonic Spectrum of stator current along with THD. AIS-SVPWM-OEWIM

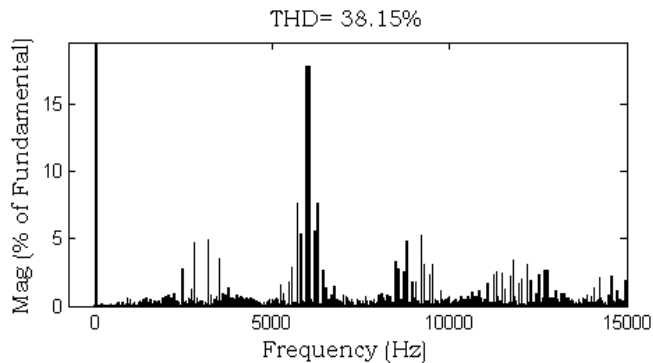


Fig 15: Harmonic Spectrum of Line voltage along with THD.

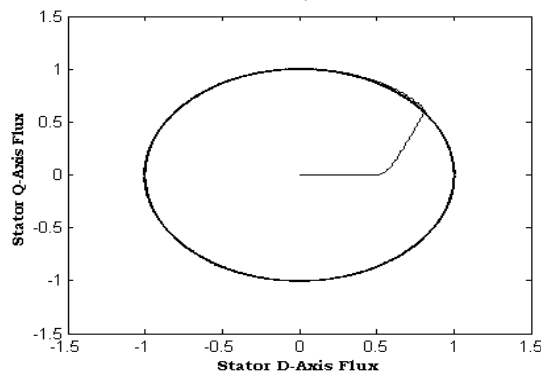


Fig 16: Locus of stator flux in AIS-SVPWM-OEWIM drive

For the comparison of the Torque, Current ripple and the THD values the conventional DTC of a Conventional induction motor drive is presented in Fig 17 and Fig 18.

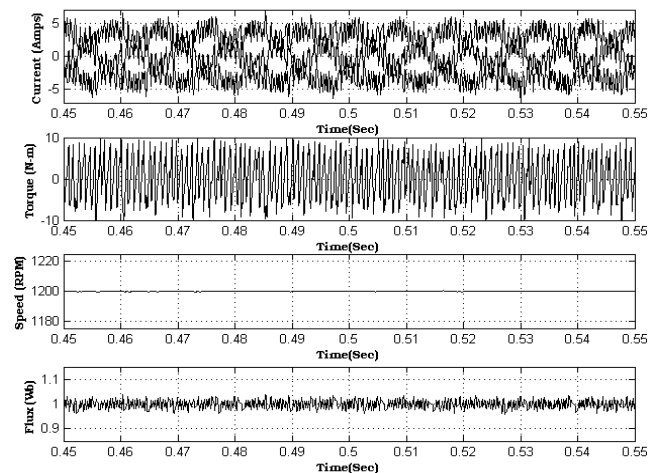


Fig 17 steady state plots of speed, torque, stator currents and stator flux for Conventional DTC based IM drive at 1200 rpm

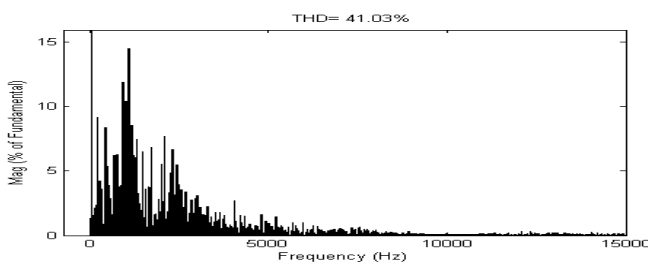


Fig 18 Harmonic Spectrum of stator current along with THD.

VI. CONCLUSION

The proposed PWM scheme uses only the three instantaneous phase reference voltages for the implementation. The control strategy proposed for reducing the switching frequency. The proposed control strategy is very simple as they do not require dividing the operating region into sub-sectors/sectors. Determining the sectors and angle of voltage vector is eliminated. The three level voltages generated using this PWM algorithm is similar to the three level voltages generated by the diode clamped inverters. With this algorithm current waveforms are superior to that of basic direct torque control scheme. The method proposed for the DTC of the Open End Winding Induction Motor gives a result in the reduction of the ripple and harmonics and distortion of stator current compare with the decoupled three level algorithms [8]. In this approach one inverter is completely clamped and other is switched therefore the two inverters share the load equally.

REFERENCES

1. EG Shivakumar, K Gopakumar, SK Sinha, VT Rangnathan, "Space Vector PWM Control of Dual Inverter Fed Open-End Winding Induction Motor Drive," IEEE-APEC, Vol.1, 2001, pp 399-405.
2. I Takahashi and T Noguchi, "A New Quick- Response and High-Efficiency Control of an Induction Motor," IEEE Trans. Industry Applications, Vol. IA-22, No.5, 1986, pp 820-827.
3. I Takahashi and Youchi Ohmori, "High- Performance Direct Torque Control of an Induction Motor," IEEE Trans. Industry Applications, Vol. IA-25, No.2, 1989, pp 257-264.
4. Janssen, M. Steimel, A. "Direct Self Control With Minimum Torque Ripple and High Dynamics for Double three-level GTO Inverter Drive," IEEE Trans. On Industrial Electronics, Vol.49, No.5, 2002, pp 1065-1071.
5. Brain A Welchko and James M Nagashima, "A Comparative Evaluation of Motor Drive Topologies for Low-Voltage, High-Power EV/HEV Propulsion Systems," IEEE International Symposium on Industrial Electronics, ISIE'03, Brazil, 2003, pp 1-6.
6. Arbind Kumar, BG Fernandes, K Chatterjee, "DTC of Open-End Winding Induction Motor Drive Using Space Vector Modulation With Reduced Switching Frequency," IEEE-PESC, 2004, pp 1214-1219.
7. Arbind Kumar, BG Fernandes, K Chatterjee, "SVPWM-DTC OF Open-End Winding Induction Motor Drive With Complete Elimination of Common Mode Voltage", Second India International Conference on Power Electronics, IICPE04, 2004,
8. G.Satheesh, T. Bramhananda Reddy and Ch. Sai Babu, "Novel SVPWM Algorithm for Open end Winding Induction Motor Drive Using the Concept of Imaginary switching Times" IJAST, Vol. 2, No.4, 2011, pp 44- 92.
9. G.Satheesh, T. Bramhananda Reddy and Ch. Sai Babu." Three Level Voltage Generation for Dual Inverter Fed Open End Winding Induction Motor drive. " IJEST, Vol. 3 No. 5 May 2011, pp 3982-3991.
10. Nabae, A., Takahashi, I., and Akagi, H.: 'A neutral-point clamped PWM inverter', IEEE- Trans. Ind. Appl., 1981, 17, (5), pp. 518-523
11. D. W. Chung, J. S. Kim and S. K. Sul, "Unified Voltage Modulation Technique for Real-Time Three-Phase Power Conversion", IEEE-Trans. on Ind.Appl, Vol.34, No.2, pp.374-380 (1998).
12. S.Srinivas and V.T.Somasekhar, "Space Vector Based PWM switching strategies for a 3 level dual inverter fed open end winding induction motor drive and their comparative evaluation" IET-Electr. Power Appl., VOL2, No.1, January 2008, PP19-31.
13. V.T. Somasekhar, MR.Baiju, KK Mohapatra and K gopakumar, "A multi level Inverter System for an Induction Motor with Open End Windings" Proc. IEEE-2002, PP 973-978
14. J.S.Kim, S.Kltage Modulation technique of the space vector PWM", IPEC Yokohama-95, pp742-747.

AUTHOR PROFILE



Sathesh. G (M'2012) was born in 1979. He graduated from Bangalore university, Bangalore in the year 2001. He received M.Tech degree from J.N.T University, Anantapur, India in the year 2004. He is presently Assistant Professor in the Electrical and Electronics Engineering Department, G. Pulla Reddy Engineering College, Kurnool, India. He is currently pursuing the Ph.D. in Electrical Engineering Department, JNTU, Kakinada. His areas of interest include Power Electronics, pulse width modulation techniques, AC Drives and Control.



Dr. T. Bramhananda Reddy (M'2010) was born in 1979. He graduated from Sri Krishna Devaraya University, Anantapur in the year 2001. He received M.E degree from Osmania University, Hyderabad, India in the year 2003. He is presently Associate Professor in the Electrical and Electronics Engineering Department, G. Pulla Reddy Engineering College, Kurnool, India. He presented more than 100 research papers in various national and international conferences and journals.



Dr. Ch. Sai Babu received the B.E from Andhra University (Electrical & Electronics Engineering), M.Tech in Electrical Machines and Industrial Drives from REC, Warangal and Ph.D in Reliability Studies of HVDC Converters from JNTU, Hyderabad. Currently he is working as a Professor in Dept. of EEE in JNTUCEK, Kakinada. He has published several National and International Journals and Conferences. His area of interest is Power Electronics and Drives, Power System Reliability, HVDC Converter Reliability, Optimization of Electrical Systems and Real Time Energy Management.